

Random Matrix Theory

Summer Project Report

Sagnik Seth

Supervisor: Dr. Anandamohan Ghosh

Contents

1	Introduction	3
1.1	Random Matrix	3
1.2	Gaussian Ensembles	3
1.3	Wigner's Semi-Circle Law	3
1.4	Wigner's Surmise	4
2	Ratio Spacing	5
2.1	Distribution of eigenvalue ratios	5
2.2	Deviation from Wigner curve	6
3	Sparse Random Matrix	7
3.1	GOE	7
3.1.1	Average Ratio Spacing	7
3.1.2	IPR	8
3.2	GUE	8
3.2.1	Average Ratio Spacing	8
3.2.2	IPR	9
4	Stochastic Processes	10
4.1	Random Walk	10
4.2	Wiener Process and Brownian Motion	11
4.3	Dyson Gas	12

1 Introduction

§1.1 Random Matrix

A matrix whose elements are random variables, sampled from some probability distribution, is called a Random Matrix. Random Matrix Theory deals with studying the properties of these matrices when the matrix dimensions become very large.

§1.2 Gaussian Ensembles

We will define two ensembles which are extensively used in study of random matrices.

Gaussian Orthogonal Ensemble (GOE)

An ensemble of $N \times N$ real matrices \mathcal{H} such that each matrix is symmetric $\mathcal{H}_{ij} = \mathcal{H}_{ji}$ and the elements of each matrix are normally distributed such that:

- $\mathcal{H}_{ij} \sim \mathcal{N}(0, 1) \forall i, j \leq N, i \neq j$
- $\mathcal{H}_{ii} \sim \mathcal{N}(0, 2) \forall i \leq N$

Alternate construction: If we take a matrix \mathcal{H} with entries from the standard normal distribution $\mathcal{N}(0, 1)$, then $\frac{\mathcal{H} + \mathcal{H}^T}{\sqrt{2}}$ is a GOE matrix.

Gaussian Unitary Ensemble (GUE)

An ensemble of $N \times N$ complex matrices \mathcal{H} such that each matrix is hermitian $\mathcal{H} = \mathcal{H}^\dagger$ and the elements are normally distributed such that:

- $\mathcal{H}_{mn} \sim \mathcal{N}(0, \frac{1}{2}) + i \mathcal{N}(0, \frac{1}{2}) \forall m, n \leq N, m \neq n$
- $\mathcal{H}_{mm} \sim \mathcal{N}(0, 1) \forall m \leq N$

Alternate construction: If we take a matrix \mathcal{H} with entries from the standard complex normal distribution $\mathcal{CN}(0, 1)$, then $\frac{\mathcal{H} + \mathcal{H}^\dagger}{\sqrt{2}}$ is a GUE matrix.

We also have Gaussian Symplectic Ensemble (GSE), constructed using quaternions, which will not be studied. We define the Dyson index β to characterise ensembles. $\beta = 1$ for GOE, $\beta = 2$ for GUE and $\beta = 4$ for GSE.

We will numerically calculate the distribution of the eigenvalues GOE/GUE. Note that since each element is a random variable, the eigenvalues are also random variables.

§1.3 Wigner's Semi-Circle Law

The limiting distribution of the eigenvalues of the Gaussian ensembles is a scaled semi-circle. Since we generally normalise our ensemble matrices to obtain eigenvalues between -1 and 1, the scaled semi-circular function takes the form:

$$f(x) = \frac{2}{\pi} \sqrt{1 - x^2} \quad (1.1)$$

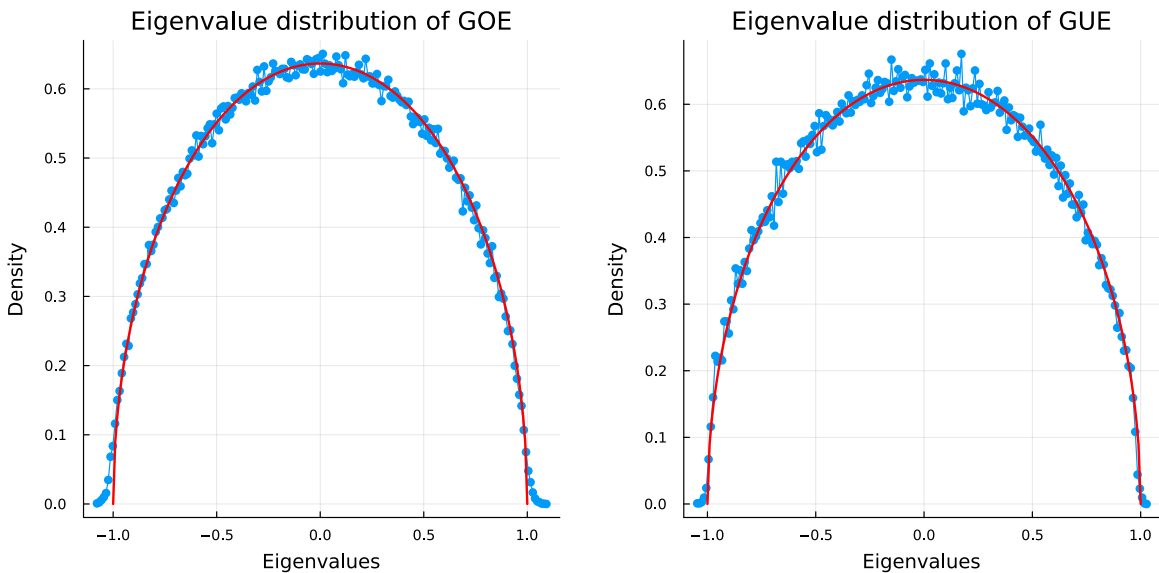


Figure 1.1: Numerically obtained eigenvalue distribution of GOE and GUE matrices of dimension $N = 100$ along with the semi-circular function.

§1.4 Wigner's Surmise

An important random variable characterising the Gaussian Ensembles is the spacing s between consecutive eigenvalues. Wigner predicted the distribution of the spacings the Gaussian ensembles. The analytic distribution of the eigenvalue spacing s for a 2×2 Gaussian ensemble matrix is given by:

$$p(s) \sim se^{-s^2/2} \quad (1.2)$$

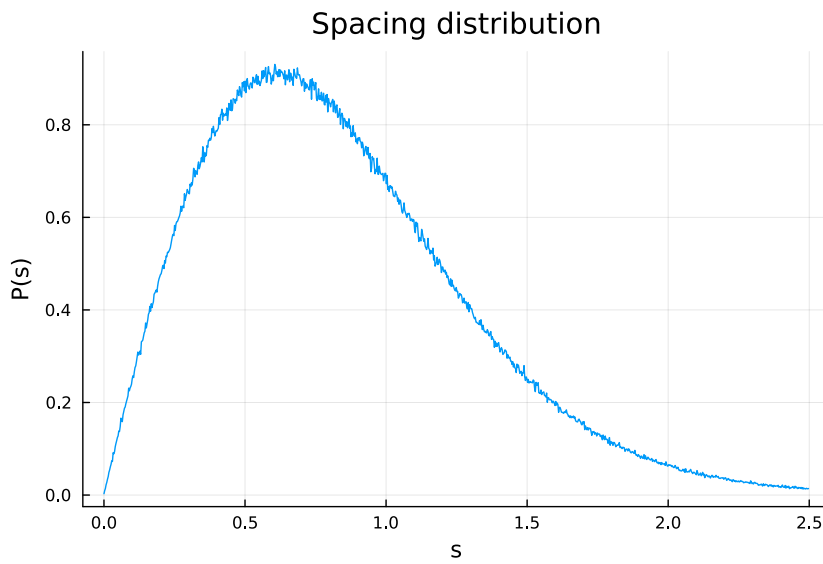


Figure 1.2: Probability distribution of level spacing

We numerically calculated the spacing distribution. We see that when $s \rightarrow 0$, we have $p(s) \rightarrow 0$. Similarly, when s becomes larger, $p(s) \rightarrow 0$. The case for large s is trivial as eigenvalues differing by a large amount should be less in number as the maximum spacing is fixed.

However, we see that the probability for finding two eigenvalues very close to each other is very less. This is termed as *level repulsion*, as two close eigenvalues (energy levels) repel each other.

2 Ratio Spacing

In the previous chapter, we plotted the eigenvalue distribution of random matrices belonging to Gaussian ensembles and also studied the spacing distribution. We will now use the distribution of another random variable which is the ratio of the consecutive eigenvalue spacings[1].

Consecutive Level Spacing

Let $\{e_n\}$ be a set of ordered energy levels and $s_n = e_{n+1} - e_n$. Then we define:

- $r_n = \frac{s_n}{s_{n-1}}$
- $\tilde{r}_n = \frac{\min(s_n, s_n - 1)}{\max(s_n, s_{n-1})}$

The analytic expression of $P(r)$ has been derived for 3×3 matrices of Gaussian ensembles and is of the form [1]:

$$P(r) = \frac{1}{Z_\beta} \frac{(r + r^2)^\beta}{(1 + r + r^2)^{1+\frac{3\beta}{2}}} \quad (2.1)$$

where β is the Dyson index and $Z_1 = \frac{8}{27}$, $Z_2 = \frac{4\pi}{81\sqrt{3}}$

§2.1 Distribution of eigenvalue ratios

We plot the distribution of r and \tilde{r} for GOE and GUE matrices. The numerical data has been obtained for matrices of dimension 1000×1000 over sufficiently large number of trials.

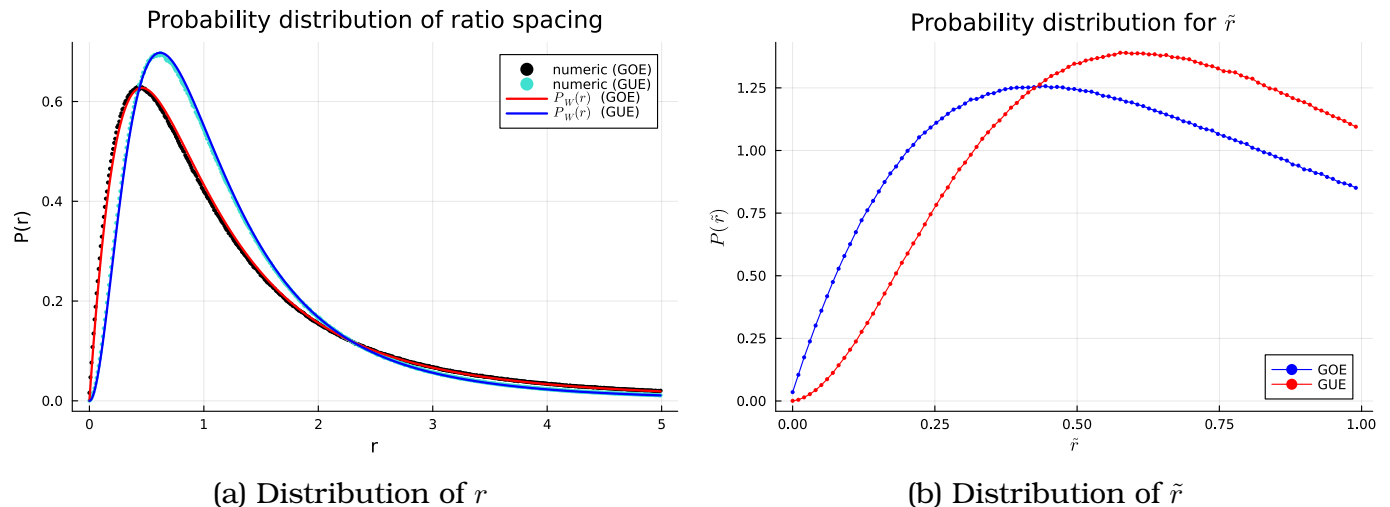


Figure 2.1: Distribution of Ratio Spacings

From the numerical data, we obtained:

- $\langle r \rangle_{GOE} = 1.778$ and $\langle r \rangle_{GUE} = 1.3684$
- $\langle \tilde{r} \rangle_{GOE} = 0.53074$ and $\langle \tilde{r} \rangle_{GUE} = 0.5997$

These values are extensively used in studies to characterise GOE and GUE matrices.

§2.2 Deviation from Wigner curve

We will now see the deviation of the numerical estimations from the analytic function of ratio spacing. We define $\delta P(r) = P_{num}(r) - P_W(r)$ where P_{num} denotes the numerical distribution and $P_W(r)$ denotes the analytic Wigner function obtained for 3×3 matrix.

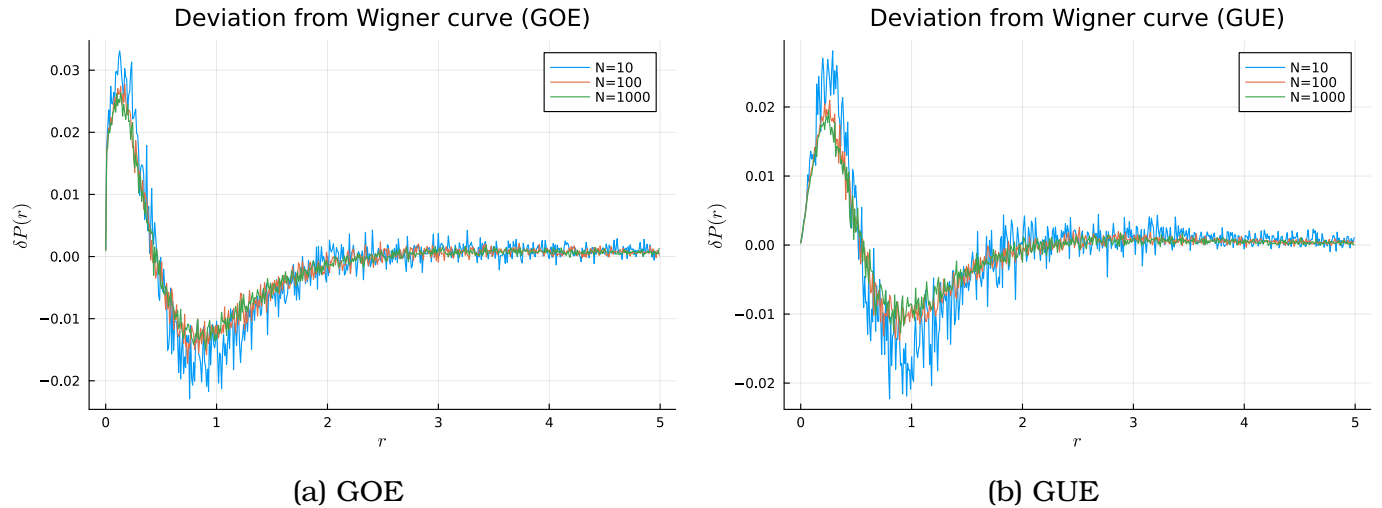


Figure 2.2: Deviation from Wigner Curve

In the plot of deviation, we can see a characteristic pattern for both GOE and GUE matrices. Initially, at $r \sim 0$, we have $\delta P(r) \sim 0$, then $\delta P(r)$ increases, reaches a maximum and then decreases, goes down below 0 and then increases again, asymptotically reaching 0 as $r \rightarrow \infty$

3 Sparse Random Matrix

Sparse Random Matrix (SRM)

A random matrix having most of its elements as zero.

We will initially start with a GOE/GUE matrix and alter its elements at each step and make them 0. This way, we will obtain a SRM starting from a Gaussian ensemble.

Algorithm

1. Take a GOE/GUE matrix \mathcal{A}
2. Define $Q = \frac{N(N-1)}{2}$
3. Choose a pair (i,j) from uniform distribution $Uniform(1, N)$. If $i \neq j$ and $\mathcal{A}_{ij} \neq 0$, then set $\mathcal{A}_{ij} = \mathcal{A}_{ji} = 0$. If not, then choose (i,j) again.
4. Repeat process P times

The above algorithm ensures that for a particular value of P, the matrix obtained at the end contains $2P$ number of zeroes as non-diagonal entries and can thus generate a sparse matrix.

We will consider the parameter $p = \frac{P}{Q}$ as a measure of sparsity of a matrix. When $p = 1$, we will obtain a matrix with only diagonal elements non-zero.

We will study the variation of $\langle \tilde{r} \rangle$ and inverse participation ratio (IPR) with the parameter p . We fine IPR by [2]:

$$IPR = \sum_{i=1}^N |\psi_i|^4$$

where ψ_i are the eigenvectors and N is the dimension for the matrix in consideration. IPR is used to study the localisation-delocalisation property of matrices.

- If there is localisation, $|\psi_i| \sim 1$ for some i and $|\psi_j| \sim 0 \forall j \neq i$. Thus, $IPR \sim 1$.
- If there is delocalisation, $|\psi_i| \sim \frac{1}{\sqrt{N}} \forall i$. Thus, $\sum_{i=1}^N |\psi_i|^4 \sim \sum_{i=1}^N \frac{1}{N^2} = N \times \frac{1}{N^2} = \frac{1}{N}$.

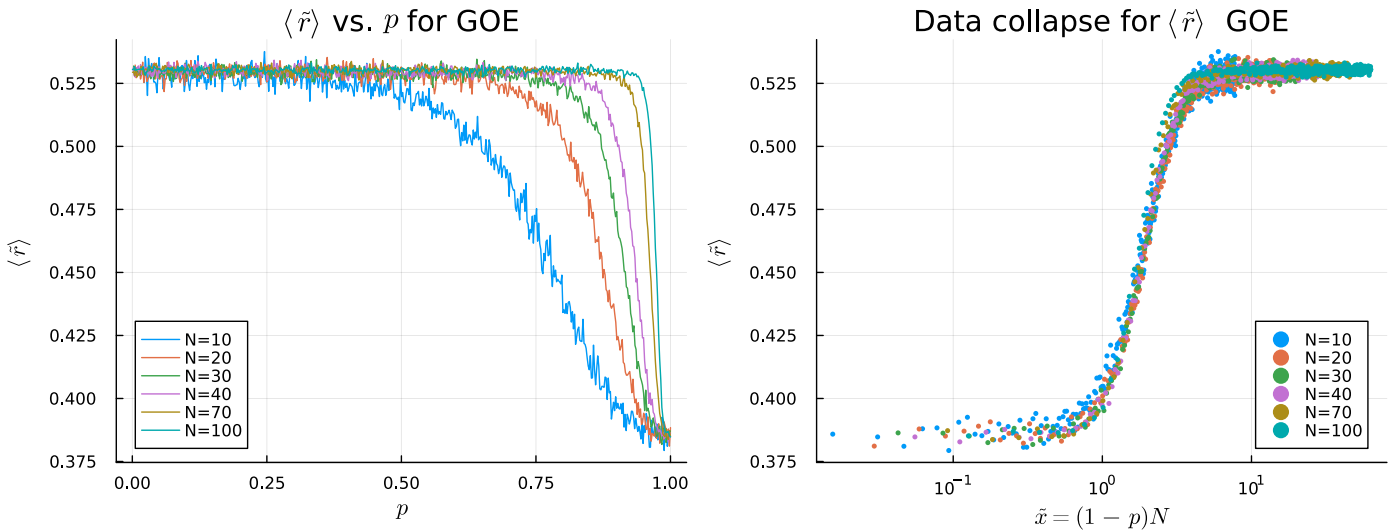
Thus, during delocalisation to localisation transition, IPR changes from 1 to N , where N is the dimension of the matrix.

§3.1 GOE

3.1.1 Average Ratio Spacing

We consider the variation of $\langle \tilde{r} \rangle$ with p for various matrix sizes. We observe that when p is close to 0, we have $\langle \tilde{r} \rangle \approx 0.53$ which is the characteristic GOE value. As p increases, we see that $\langle \tilde{r} \rangle$ approaches approximately to 0.386 which is the characteristic Poisson value.

3 Sparse Random Matrix



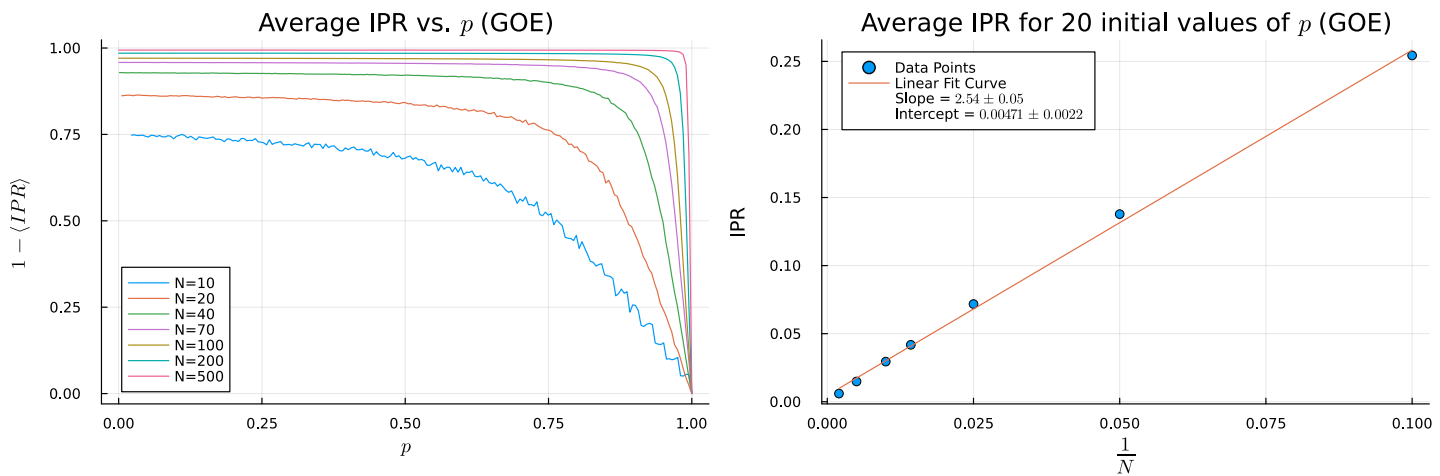
We also tried to obtain an approximate data collapse for $\langle \tilde{r} \rangle$ for different matrix dimensions. It was seen that if we rescale our x-axis as $(1 - x)N$, we obtain a data collapse (where N is the dimension of the matrix in consideration). Thus, we can say:

$$\boxed{\langle \tilde{r} \rangle_{GOE} \sim f((1 - p)N)} \quad (3.1)$$

where f is an universal function.

3.1.2 IPR

We will also consider the variation of IPR with p for various matrix sizes.

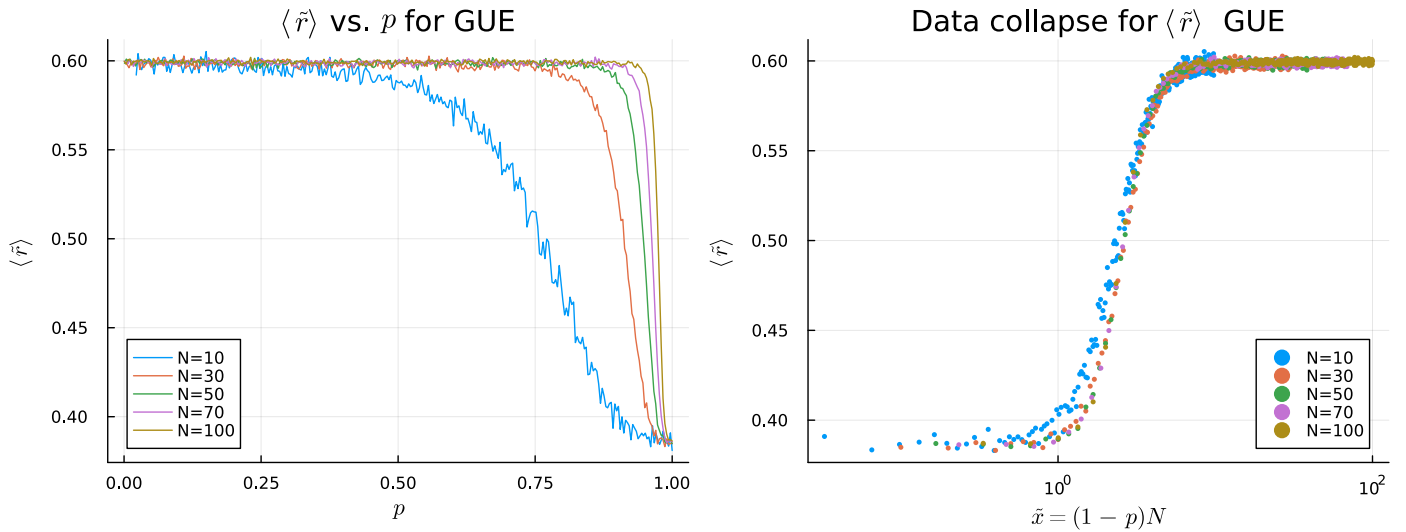


§3.2 GUE

3.2.1 Average Ratio Spacing

We repeat the same process for GUE matrices. Similar to the GOE case, we find that $\langle \tilde{r} \rangle$ is initially around 0.6 which is the characteristic GUE value. As p increases, $\langle \tilde{r} \rangle$ decreases to around 0.386 which is the characteristic Poisson value.

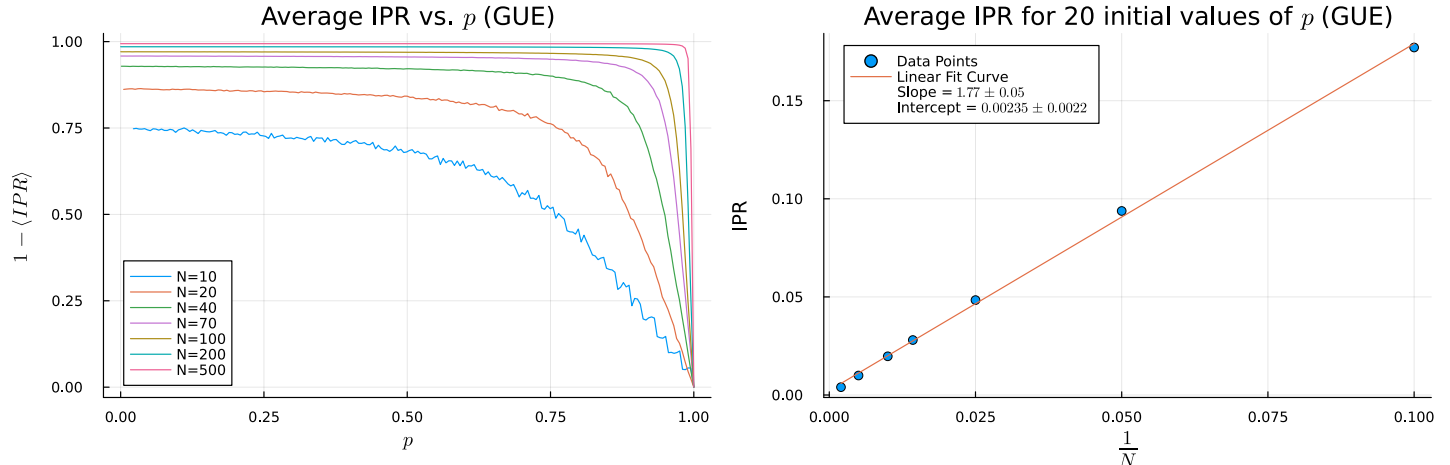
3 Sparse Random Matrix



Here also we rescale our x-axis as $(1 - p)N$ and obtain an approximate data collapse. Thus, we can say:

$$\langle \tilde{r} \rangle_{GUE} \sim \tilde{f}((1 - p)N) \quad (3.2)$$

3.2.2 IPR



Both $\langle \tilde{r} \rangle$ and IPR show delocalisation to localisation transition as p increases.

4 Stochastic Processes

In this chapter, we will consider random processes which are a sequence of random variables where the indices of the sequence are interpreted as time. We will consider processes pertaining to random matrices. Specifically, we will analyse the model of Dyson's Coulomb Gas.

§4.1 Random Walk

Discrete Random Walk

Let X_0 be an initial position and $\{P_n\}$ be sequence of iid random variables. Then we can define a random walk by:

$$X_n = X_{n-1} + P_n \quad n \geq 1 \quad (4.1)$$

For a 1D random walk, we usually take P_n such that $P_n \in \{-1, +1\}$. Hence, each step, the walker position increases or decreases by 1. Random walks are an example of Markov processes where subsequent position depend only on the present position of the walker.

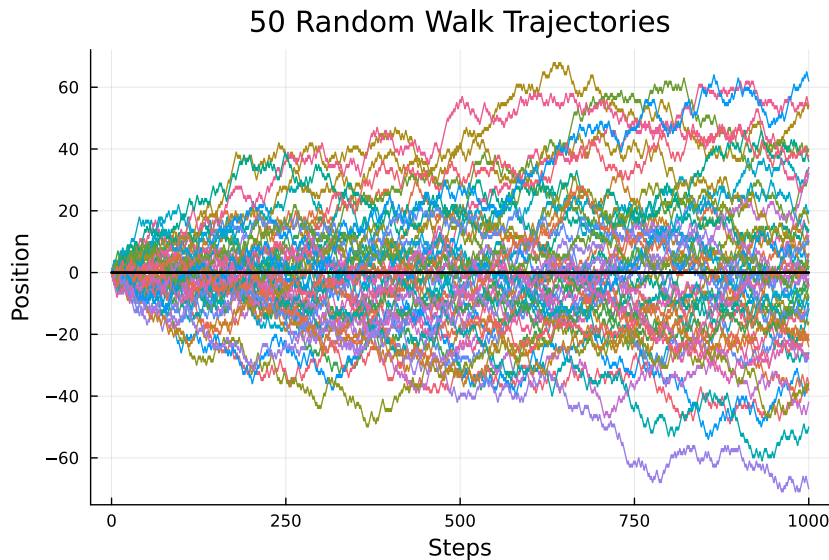


Figure 4.1: Trajectories of 50 random walks, all starting from initial position 0.

In the above figure, we see the trajectories of different walkers starting from same position. During the different time steps, we see that the position of one walker is independent of the other. Thus, the walkers intersect at many time steps.

§4.2 Wiener Process and Brownian Motion

Wiener Process

Let Σ be a set of times. Then a stochastic process $\{W_t\}_{t \in \Sigma}$ such that:

- $W_0 = 0$ almost surely.
- The map $t \mapsto X_t$ is continuous function in Σ almost surely.
- W has independent Gaussian increments, that is, $W_{t+dt} - W_t \sim \mathcal{N}(0, dt)$

The Brownian motion is a type of Wiener process which is used to describe the random motion of particles suspended in a medium.

Symmetric Brownian Motion

A matrix process S_t of symmetric matrices, whose entries are the independent Brownian motions.

$$S_t^{ij} = \begin{cases} \frac{1}{\sqrt{d}} B_t^{ij} & i \neq j \\ \sqrt{\frac{2}{d}} B_t^{ii} & i = j \end{cases} \quad (4.2)$$

The symmetric Brownian motion consists of a symmetric matrix, each of whose elements perform Brownian motions independently, constrained only by the symmetry condition.

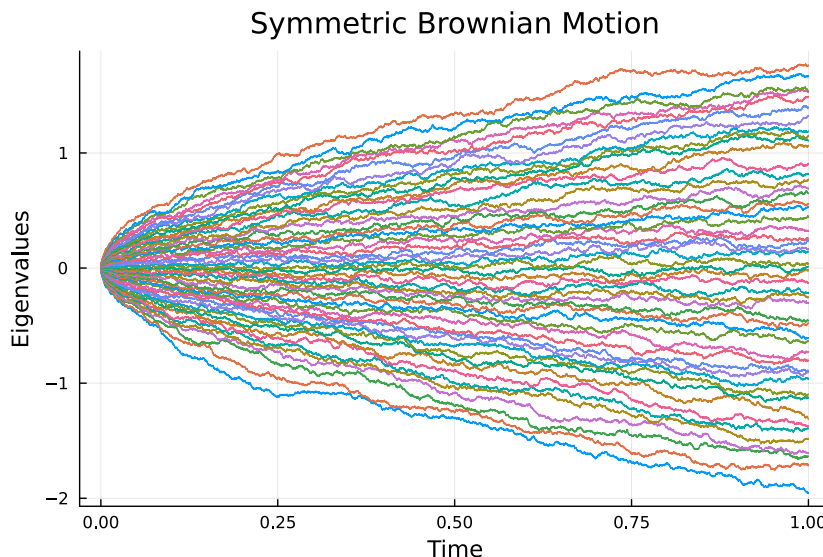


Figure 4.2: Simulation of a Symmetric Brownian motion of a matrix of dimension $d = 50$

When we consider the time evolution of the eigenvalues, we find that the eigenvalues ‘spread out’ as time progresses and never intersect each other. Moreover, if at one instant, two eigenvalues become very close, there is repulsion and hence during the next time step, these eigenvalues move away from each other.

Modified Symmetric Brownian Motion

We will construct a modified SBM, with parameter p . With probability p , the symmetric off-diagonal terms S_t^{ij} and S_t^{ji} , $i \neq j$, will be set to 0, for all times t .

Thus, in the modified SBM, for low p , the process will evolve as unmodified SBM model which will be GOE-like process and for high p , we will have only the diagonal terms remaining, thus the model will evolve as a Poisson process.

We plot the variation of $\langle \tilde{r} \rangle$ vs. p for the modified SBM.

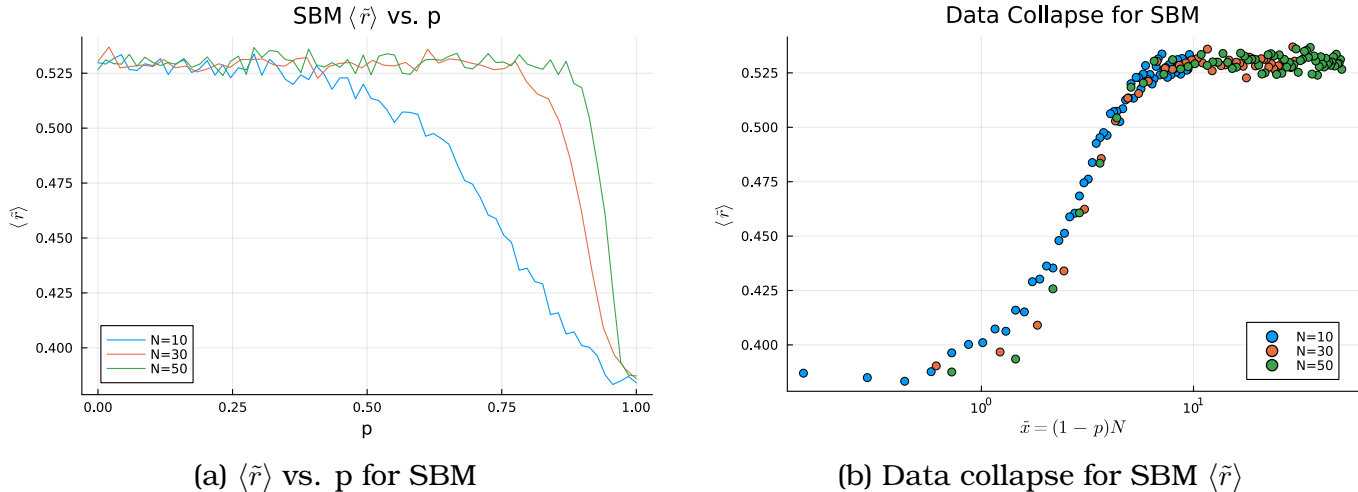


Figure 4.3: Modified SBM simulation with p , for varying system size

We can observe that the variation is similar to what we obtained in the case for sparse random matrix. We again used our previous scaling for the x-axis $\tilde{x} = (1 - p)N$ to obtain the data collapse.

§4.3 Dyson Gas

Dyson Gas

A collection of particles performing independent Brownian motions, under the action of mutual repulsion.

The Dyson Gas evolves according to the following model:

$$P_{t+dt}^i = P_t^i + \sqrt{\frac{2dt}{d}} \mathcal{N}(0, 1) + \frac{1}{d} \sum_{1 \leq j \neq i \leq d} \frac{dt}{P_t^i - P_t^j} \quad (4.3)$$

where P_t^i denotes the position of the i^{th} particle at time t . The last term is the *repulsion term* which prevents the particle from coming close to each other. Due to the repulsion term, the Dyson Gas is not typically a Wiener process.

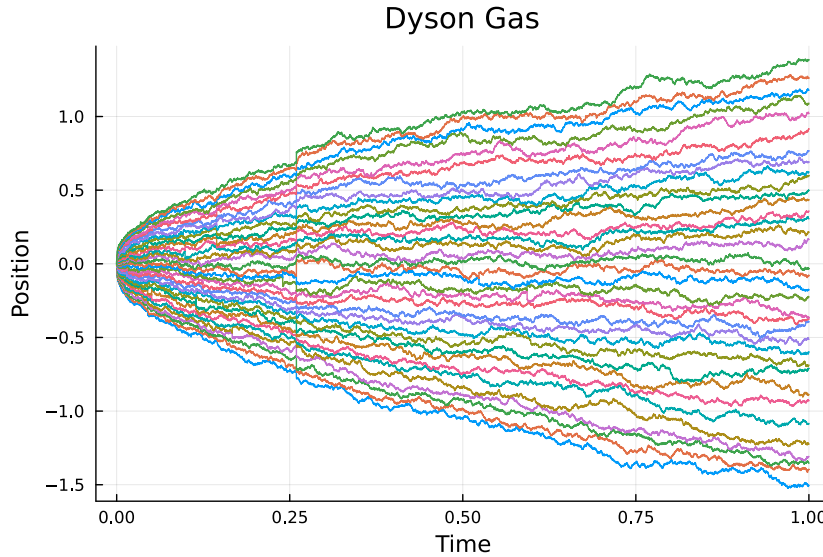


Figure 4.4: Simulation of a Dyson Gas for $d = 50$ particles

We started with an initial array with normally distributed random variables with very small standard deviation ($\sigma \approx 10^{-4}$). The simulation is numerically unstable, specially for the particles on the edge, since the repulsion term can take large values at some time. We have omitted a few of the edge particles' position. The resulting figure resembles that of *Symmetric Brownian Motion*[3].

Here, we have taken the positions of the particles as equivalent to the eigenvalues and we calculated $\langle \tilde{r}(t) \rangle$, and found that the system equilibrated at $\langle \tilde{r} \rangle_{eq} \approx 0.56$.

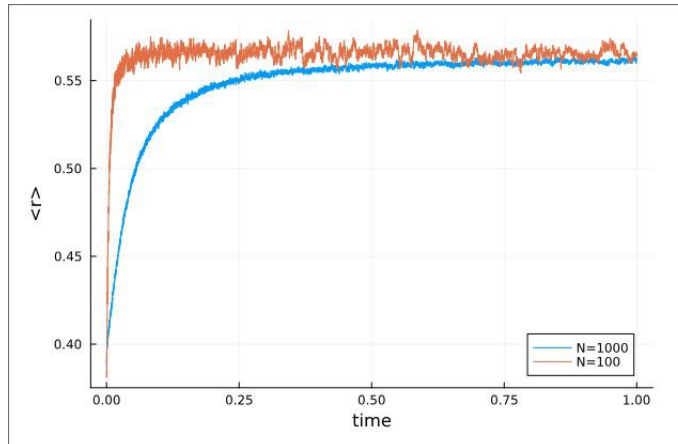


Figure 4.5: Variation of $\langle \tilde{r} \rangle$ with time for $N=100, 1000$ particles.

We know that $\langle \tilde{r} \rangle_{GOE} \approx 0.53$. Thus, the Dyson Gas approximates a GOE process. The deviation from the typical GOE value might occur due to the numerical instability of the repulsion term.

Modified Dyson Gas

We introduce a coupling term J_{ij} in the model for Dyson Gas and modify it to approximate different Gaussian ensembles processes by incorporating Dyson index β .

$$P_{t+dt}^i = P_t^i + \sqrt{\frac{2dt}{\beta d}} \mathcal{N}(0, 1) + \frac{1}{d} \sum_{1 \leq j \neq i \leq d} \frac{J_{ij} dt}{P_t^i - P_t^j} \quad (4.4)$$

where, $J_{ij} = 0$ with probability p and $J_{ij} = 1$ with probability $1 - p$ and β is the Dyson index.

The modification restricts the number of particles to which a particle is coupled. For high p , we have $J_{ij} = 0$, thus, there is lesser coupling between the particles and the system evolves such that the process is Poisson-like. For low p , we have $J_{ij} = 1$, hence we obtain our original Dyson Gas system and the process is GOE-like for $\beta = 1$ and GUE-like for $\beta = 2$.

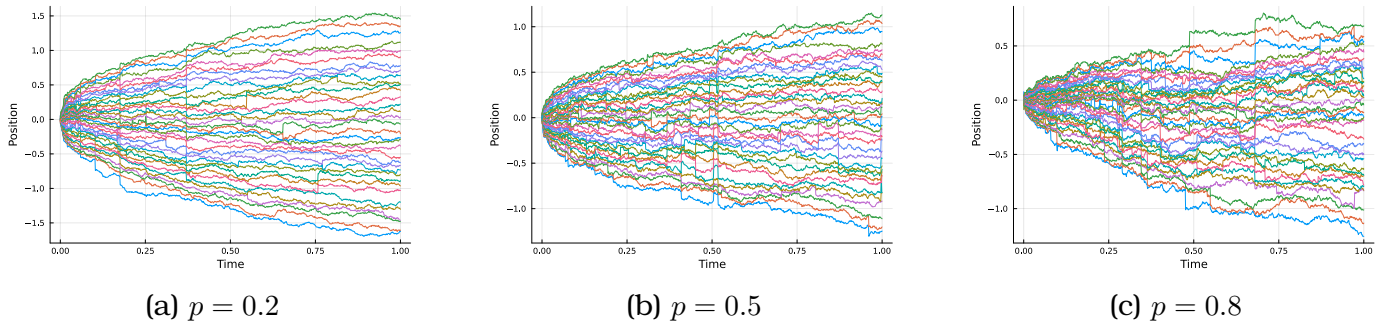


Figure 4.6: Modified Dyson Gas simulation for different values of p ; $N=60$ particles, $\beta = 1$

$\beta = 1$: GOE-like evolution

We obtained the variation of $\langle \tilde{r} \rangle$ with p numerically. The variation is consistent with our expectation to how we defined the model.

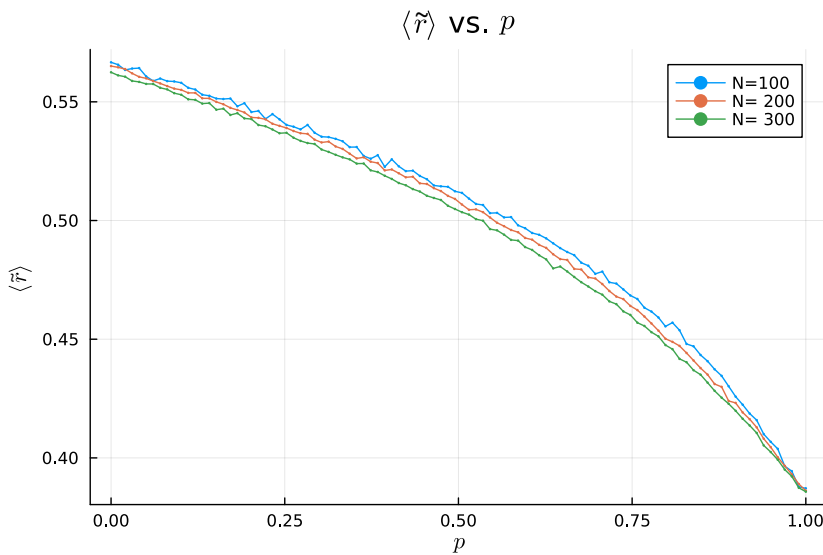


Figure 4.7: $\langle \tilde{r} \rangle$ variation with p for $N = 100, 200, 300$. The average was calculated at $t = 2$, $dt = 0.001$, for 1000 trials,

We can see that the variation for $\langle \tilde{r} \rangle$ with p was similar for different values of N . Initially $\langle \tilde{r} \rangle \approx 0.56$ which is what we obtained previously, denoting a GOE-like process. Finally, we have $\langle \tilde{r} \rangle \approx 0.386$ which is a characteristic of Poisson process. Thus, there is transition from Poisson to GOE as p increases.

We note that the dependence of $\langle \tilde{r} \rangle$ on the number of particles is not prominent unlike the case in the sparse random matrix where the variation of $\langle \tilde{r} \rangle$ with p was different for different matrix dimensions. To verify this, we plot $\langle \tilde{r} \rangle$ with varying number of particles N for different values of p .

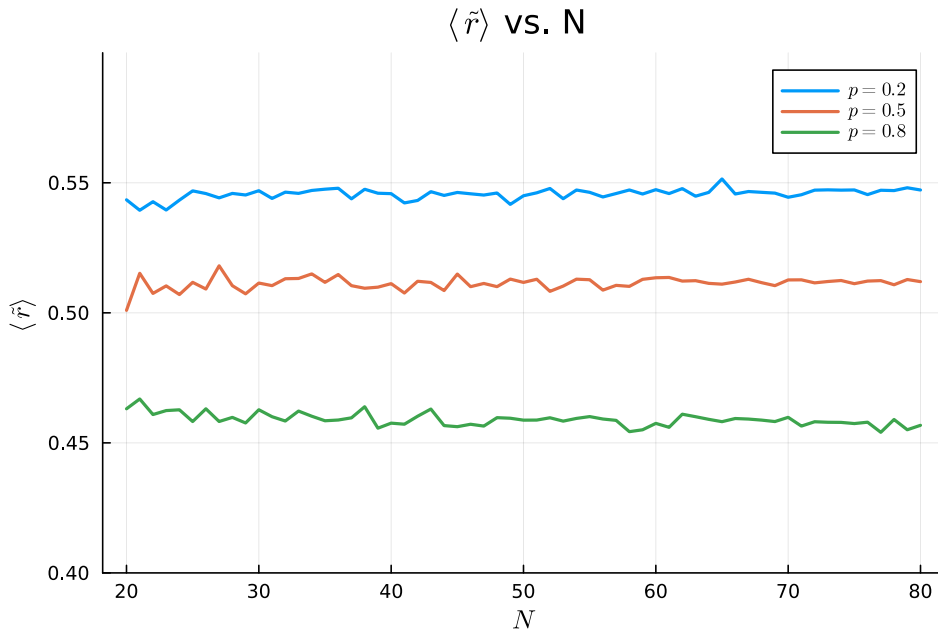


Figure 4.8: $\langle \tilde{r} \rangle$ variation with number of particles for $p = 0.2, 0.5, 0.8$; $\beta = 1$

We can see that $\langle \tilde{r} \rangle$ remains almost constant with minor fluctuations for increasing values of N , indicating that $\langle \tilde{r} \rangle$ is independent of system size unlike the case of SRM.

$$\boxed{\beta = 2 : \text{GUE-like evolution}}$$

We do the same analysis for GUE-like evolution of the Dyson Gas.

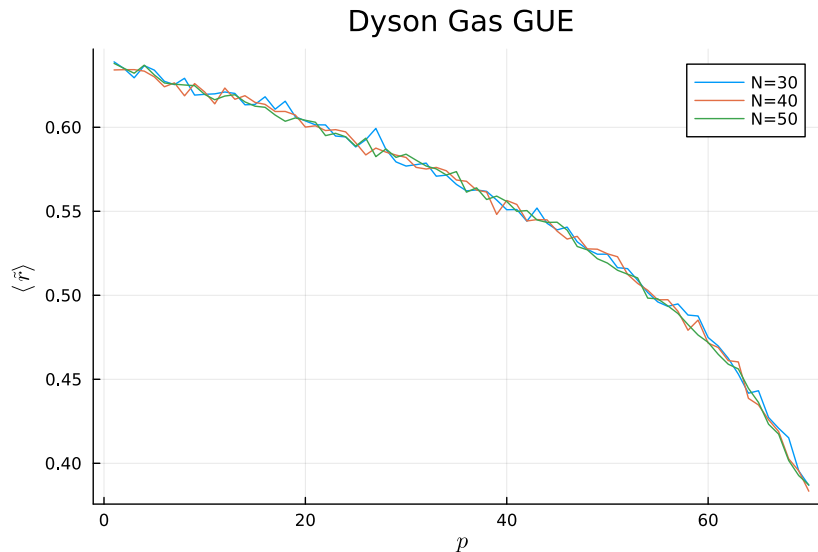


Figure 4.9: $\langle \tilde{r} \rangle$ variation with p for $N = 30, 40, 50$.

We again see that $\langle \tilde{r} \rangle \approx 0.63$ for lower p which is close to the characteristic GUE value of 0.6, thus the process is GUE-like. For higher p , $\langle \tilde{r} \rangle \approx 0.38$, thus the process is Poisson-like. Similar to the previous case, the variation of $\langle \tilde{r} \rangle$ is apparently size-independent.

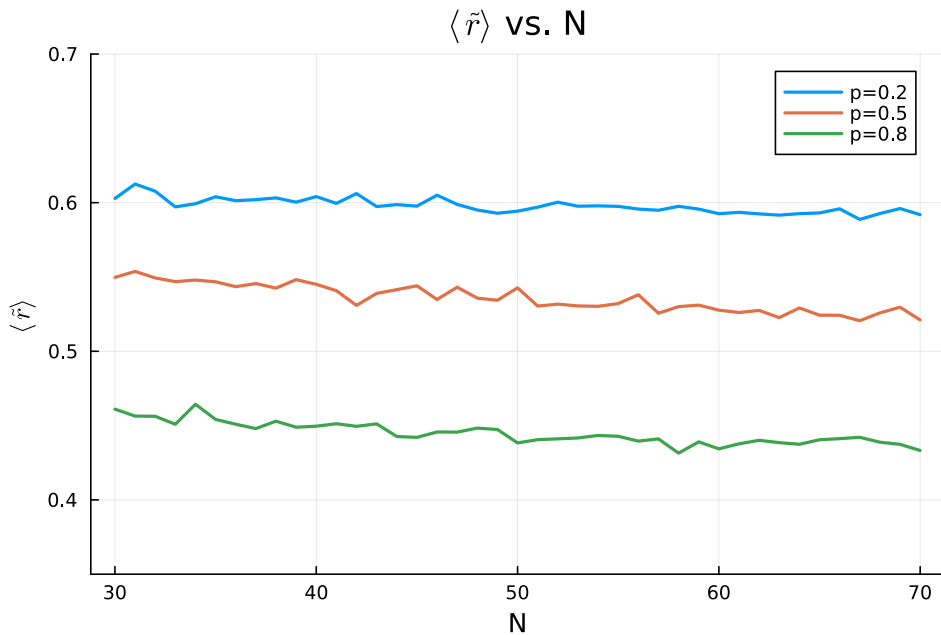


Figure 4.10: $\langle \tilde{r} \rangle$ variation with number of particles for $p = 0.2, 0.5, 0.8$; $\beta = 2$

Bibliography

- [1] Y. Y. Atas, E. Bogomolny, O. Giraud, and G. Roux. Distribution of the ratio of consecutive level spacings in random matrix ensembles. *Phys. Rev. Lett.*, 110:084101, Feb 2013.
- [2] S. N. Evangelou. A numerical study of sparse random matrices. *Journal of Statistical Physics*, 69(1):361–383, Oct 1992.
- [3] Gianluca Finocchio. Random matrix theory: Dyson brownian motion. *Snapshots of modern mathematics from Oberwolfach*, 2020.